

## **General Disclaimer**

### **One or more of the Following Statements may affect this Document**

- This document has been reproduced from the best copy furnished by the organizational source. It is being released in the interest of making available as much information as possible.
- This document may contain data, which exceeds the sheet parameters. It was furnished in this condition by the organizational source and is the best copy available.
- This document may contain tone-on-tone or color graphs, charts and/or pictures, which have been reproduced in black and white.
- This document is paginated as submitted by the original source.
- Portions of this document are not fully legible due to the historical nature of some of the material. However, it is the best reproduction available from the original submission.



## Technical Memorandum 79611

# Inference of the Ring Current Ion Composition by Means of Charge Exchange Decay

**Paul H. Smith, N. K. Bewtra,  
and R. A. Hoffman**

(NASA-TM-79611) INFERENCE OF THE RING  
CURRENT ION COMPOSITION BY MEANS OF CHARGE  
EXCHANGE DECAY (NASA) 41 p HC A03/MF A01

CSSL 20L

N78-32898

Unclas  
33093

G3/76

**AUGUST 1978**

National Aeronautics and  
Space Administration

**Goddard Space Flight Center**  
Greenbelt, Maryland 20771



INFERENCE OF THE RING CURRENT ION COMPOSITION  
BY MEANS OF CHARGE EXCHANGE DECAY

Paul H. Smith  
Laboratory for Planetary Atmospheres  
NASA/Goddard Space Flight Center  
Greenbelt, Maryland 20771

N. K. Bewtra  
Computer Sciences Corporation  
Silver Spring, MD 20910

R. A. Hoffman  
Laboratory for Planetary Atmospheres  
NASA/Goddard Space Flight Center  
Greenbelt, Maryland 20771

## ABSTRACT

The analysis of data from the Explorer 45 (S<sup>3</sup>-A) electrostatic analyzer in the energy range 5 to 30 keV has provided some new results on the storm time ring current ion composition. It has been well established that the storm time ring current has a decay time of several days during which the particle fluxes decrease nearly monotonically. In the past ring current studies have assumed or stated that hydrogen was the dominant ion in the earth's ring current. By analyzing the measured ion fluxes during the several day storm recovery period and assuming that beside hydrogen other ions were present and that the decays were exponential in nature, we were able to establish three separate lifetimes for the ions. These fitted decay lifetimes are in excellent agreement with the expected charge exchange decay lifetimes for H<sup>+</sup>, O<sup>+</sup>, and He<sup>+</sup> in the energy and L-value range of the data. This inference technique, thus, establishes the presence of measurable and appreciable quantities of oxygen and helium ions as well as protons in the storm-time ring current; we also find indications that He<sup>++</sup> may also be present under these same conditions.

## INTRODUCTION

Since the early suggestion of Dessler and Parker (1959) that the charge exchange mechanism could be significant in the ring current decay process, this mechanism has varied between being in favor and out of favor in explaining ring current particle decay after magnetic storms. The long term decay times of several days for the measured fluxes were consistent with the available charge exchange lifetimes and, therefore, supported the charge exchange position (Frank, 1967; Swisher and Frank, 1968). These favorable comparisons were based on the early computational work by Liemohn (1961), who specified both the mean lifetime,  $\tau_e$ , for protons confined to the equatorial plane and the charge exchange lifetime,  $\tau_m$ , for protons mirroring off the geomagnetic equator. More recently, other theoretical and observational aspects, such as the emergence of wave-particle theory (Cornwall et al., 1970) and the discrepancy pointed out by Lyons and Evans (1976) between the observed proton pitch angle distributions and those predicted by charge exchange decay weakened the charge exchange position. It also became apparent that the overall measured decay lifetimes no longer agreed well with the more recently computed values (Prölss, 1973; Tinsley, 1976).

Smith et al. (1976) were among the first to use charge exchange lifetime values modified from those given by Liemohn (1961) for comparison to their satellite measurements. They employed both the neutral hydrogen density,  $n$ , of Prölss (1973) and the proton charge exchange cross section,  $\sigma$ , of McClure (1966). Lyons and Evans (1976) used the equatorial charge exchange lifetimes given by Tinsley (1976), whose values were also a modification due to a better determination of the neutral hydrogen density

and charge exchange cross sections. Additional progress was made by Smith and Bewtra (1976) and independently by Cowley (1977) in recomputing the relationship between the lifetimes of equatorially mirroring particles and those particles mirroring off the geomagnetic equator. Their results showed that the off-90° pitch angle ion fluxes would not charge exchange decay as rapidly as was previously thought. In the review of the recent work associated with the determination of the charge exchange lifetimes for various ions in the magnetosphere, Smith and Bewtra (1977) provide the updated and corrected lifetime values especially through the ring current region. While this area of space research has been experiencing some recent controversy over the various mechanisms, there is no question but that our understanding of the ring current source and loss mechanisms is progressing in a significant manner.

In this paper we examine the consequences of making the assumption that, besides protons, ions such as helium and oxygen can represent a major fraction of the storm-time ring current particle flux. All of the improvements and new measurements in determining the charge exchange lifetimes (Smith and Bewtra, 1977) are used. The charge exchange decay mechanism then is used to infer the ion composition in the ring current during the recovery phase of geomagnetic storms.

## Background

Until the recent work by Lyons and Evans (1976) and Tinsley (1976), in which they suggest  $\text{He}^+$  as a significant ion, ring current studies have assumed or stated that hydrogen was the dominant ion composing the ring current (Berko et al., 1975; and others before that). However,  $\text{O}^+$  ions have been shown to be the dominant ion species under geomagnetic storm-time conditions at low altitudes (Shelley et al., 1972; Sharp et al., 1976a,b). Shelley et al. (1976) report new observations of  $\text{O}^+$  and  $\text{H}^+$  fluxes streaming up the field lines from the ionosphere and Johnson et al. (1977) report observations of  $\text{H}^+$ ,  $\text{He}^+$  and  $\text{O}^+$  in the ring current L-values at altitudes of 5000-7000 km. Indirect evidence of  $\text{O}^+$  at higher altitudes has been offered by McIlwain (1976) from observations at synchronous orbit on ATS-6 and by Frank et al. (1977) from IMP-7 at much larger altitudes near the geomagnetic tail.

In this paper we present the analysis of data from the Explorer 45 ( $\text{S}^3\text{-A}$ ) electrostatic analyzer. This analyzer system measured the total ion flux in the energy per unit charge range of 1 to 30 keV. Smith et al. (1976) used measurements from this same instrument in a previous analysis. Assuming that the instrument was responding primarily to protons, the observed flux decay rates during the February 24, 1972, magnetic storm recovery generally agreed with the predicted charge exchange decay rates available at that time. There were, however, several difficulties. First, the observed decay rates, while in good agreement with those predicted by Liemohn (1961), were longer than the newer predicted proton decay rates given by Prölss (1973). Second, the ordering of the data at

L = 3.5 was not as good as it was at the higher L-values of 4.25 and 5.0. Third, the off-90<sup>0</sup> pitch angle particles did not decay as rapidly as proton charge exchange would have predicted (Liemohn, 1961).

Based on the work by Smith and Bewtra (1976) regarding the predicted pitch angle dependence for the charge exchange decay mechanism and on the revised charge exchange lifetime values reviewed by Smith and Bewtra (1977), the Explorer 45 measurements have been re-analyzed. The following new procedures were employed:

1. Only those particles having the same equatorial pitch angle were considered within a given data subset. Even with a near geographic equatorial orbit (3<sup>0</sup> inclination), the Explorer 45 satellite does vary in magnetic latitude from orbit to orbit due to the 11<sup>0</sup> offset of the earth's magnetic field axis (see Figure 7, Smith et al., 1976). This meant that for those off-geomagnetic-equator orbits, fluxes measured at 90<sup>0</sup> local pitch angle did not mirror at  $\lambda_m = 0^0$ . In order to have a measurement every orbit (7.8 hrs.) at the same L-value and local time,  $\lambda_m = 14^0$  was the smallest mirror latitude which could be used. A dipole geomagnetic field is assumed for all the calculations in this paper.
2. For the normal sampling rate of the electrostatic analyzer and the satellite spin period, two consecutive readouts corresponded roughly to pitch angles about 12<sup>0</sup> apart. These two readouts were linearly interpolated to obtain the particle flux at the required pitch angle. Further, to reduce the statistical uncertainties, this process was repeated for the next such set of readouts for the same energy (usually a minute later) and the two calculated fluxes were averaged to obtain the flux at the specified L-value.

3. The neutral hydrogen density was determined individually for each of the geomagnetic storms considered. The geophysical conditions (solar activity, magnetic activity, season, etc.) for the specific time periods were used in this process. Smith and Bewtra (1977) provide the detailed description of this procedure.
4. It was assumed that more than one ion species could be present in measurable quantities in the ring current region after these geomagnetic storms. The measured flux decay data were fitted with a double or triple exponential decay function of the form:

$$f = \sum_i \alpha_i e^{-(t/\tau_i)} \quad (1)$$

where the  $\alpha_i$ 's are the fitted variables representing the relative quantities of each of the ion species,  $t$  is the time after the decay process begins, and the  $\tau_i$ 's are the fitted variables representing the decay lifetime for each of the assumed ion species. In the functional fitting process the  $\alpha_i$ 's and  $\tau_i$ 's were all free variables with no assumption made as to which specific ions were involved.

5. The entire ring current recovery period was considered from the maximum of the main phase to the time at which either the AE index or Dst was again enhanced by a disturbance. This will be discussed later in more detail.

## FLUX DECAY OBSERVATIONS

### Magnetic Storm Conditions

Ion measurements from the Explorer 45 ( $S^3$ -A) electrostatic analyzer made during three geomagnetic storms are presented in this section. Two of the storms, one beginning on February 24, 1972, and the other beginning on May 15, 1972, were moderate storms with maximum negative Dst (M. Sugiura and D. J. Poros, private communication, 1973) of around  $75\gamma$  (Figures 1a and 1b). Cahill and Lee (1975) have described some of the Explorer 45 magnetic field observations during the February storm. The third storm is the large, well known December 17, 1971, magnetic storm (Cahill, 1973) with a maximum negative Dst of  $171\gamma$  (Figure 1c). The AE index provides a quantitative measure of the auroral zone magnetic activity produced by enhanced ionospheric currents flowing below and within the auroral oval (Allen et al., 1975). The trajectories of the satellite orbit for the three magnetic storms are shown in Figure 2. The magnetic local time (MLT) of apogee varied from 2100 MLT during the December storm to 1700 MLT during the May storm.

The measured ion fluxes at an energy of 9.2 keV and an L-value of 4.25 outbound are shown in Figure 3 for the three storms for five or six day periods, which include the storm commencements, main phase maxima and the long recovery phases. Only those particles which mirrored at the same geomagnetic latitude of  $\lambda_m = 14^\circ$  were selected. The equatorial pitch angle corresponding to this mirror latitude is about  $61.3^\circ$ .

In the February and May storms the particle fluxes at this energy increased nearly an order of magnitude after the sudden commencement and

did so within the 8 hours between one orbit and the next. Within this resolution the maximum observed flux was reached nearly simultaneously with the maximum of the main phase of the storm. The particle flux then decayed monotonically over the next several days until new magnetic activity occurred, at which time the particle flux again increased. In the December storm a similar pattern occurred with the exception of the initial period after the main phase maximum. The extended period of "storm-related activity" (shown in Figure 3) was a result of large substorms occurring in conjunction with the principal main phase storm on December 17. This substorm activity can be identified from the AE index in Figure 1. It is interesting to note, however, that there was observed in the "storm-related activity" period a general reduction in particle flux for about a day and a half before a flux increase occurred again on December 19. The AE index (Figure 1) increased on this day to over  $700\gamma$ . A period of "new activity" occurred on December 22 as is evidenced by a flux increase (Figure 3) and by the AE and Dst activity (Figure 1) during this day.

The following sequence of events is evident for these storms: 1) A period of principal storm-related activity occurred on a variable time scale depending on the specific geomagnetic storm, during which the ring current particle flux increased significantly and during which subsequent substorm injections may have kept the observed flux levels from decreasing in an unimpeded way; 2) next a decay period occurred during which new particle injections appeared to be negligible; 3) finally, new particle injections terminated the relatively quiet decay period. In the following, we shall be considering primarily the "decay period" as indicated in Figure 3.

## Application of Charge Exchange Delay

The improved charge exchange lifetimes given by Smith and Bewtra (1977) were used to determine the specific charge exchange lifetimes,  $\tau$ , for various ions at L-values and energies of interest. These values reflect the best determination of the cross sections, neutral hydrogen density and mirror latitude dependence which are available as well as inputs of the specific geophysical conditions during the Explorer 45 observations. These inputs are given in Table 1 (items 1-8) for the three magnetic storm periods. The detailed definitions of the density and temperature at the exobase,  $N_C$  and  $T_C$ , respectively, and the satellite critical altitude,  $R_{SC}$ , are reviewed also by Smith and Bewtra (1977). Under the stated conditions in Table 1 (items 1-9) the neutral hydrogen densities  $n$ , were computed for the three storms and are given in item 10.

For the ions  $H^+$ ,  $O^+$ ,  $He^+$  and  $He^{++}$  Figure 4 shows the normalized flux decay expected to be observed assuming only charge exchange decay and using the February, 1972, magnetic storm conditions. Ion energies of 6.0, 9.2, 13.5 and 25.6 keV, and L-values of 3.5, 4.25 and 5.0 are considered for the ions which are assumed to be mirroring at  $\lambda_m = 14^\circ$ . In this paper we use the mass 4 isotope of the helium ions. For the singly charged ions, as can be seen from Figure 4, there are significant and potentially observable differences in the expected fluxes after 2-3 days of decay. In the electrostatic analyzer doubly charged ions, such as  $He^{++}$ , will be detected and recorded at energies which are half their actual energies. Therefore, to display the appropriate  $He^{++}$  separation the charge exchange lifetimes used are for energies twice those shown. As can be seen in Figure 4 the  $He^{++}$  lifetimes are not different enough from  $H^+$  at all of these energies to always permit a separation of these two ions.

TABLE 1: STORM PARAMETERS FOR CHARGE EXCHANGE DECAV

Parameter	Dec. 17, 1971	Feb. 24, 1972	May 15, 1972
1. $A_p$	11-19 (in 2 $\gamma$ )	16-33 (in 2 $\gamma$ )	17-21 (in 2 $\gamma$ )
2. $f_{10.7}$ flux	133.8-143.8 ( $10^{-22}W/m^2Hz$ )	152.3-167.7 ( $10^{-22}W/m^2Hz$ )	153.0-161.1 ( $10^{-22}W/m^2Hz$ )
3. 81 day mean of $f_{10.7}$	117.8	128.4	126.0
4. Local time	Assume symmetric	Assume symmetric	Assume symmetric
5. Geographic Latitude	Assume equatorial	Assume equatorial	Assume equatorial
6. $N_C$	$8.0 \times 10^4/cm^3$	$6.5 \times 10^4/cm^3$	$7.0 \times 10^4/cm^3$
7. $T_C$	$970^0K$	$1024^0K$	$1005^0K$
8. $R_{SC}$	$2.5 R_C$	$2.5 R_C$	$2.5 R_C$
9. L-value	4.25	4.25	4.25
10. Density, n	$204/cm^3$	$219/cm^3$	$203/cm^3$

The charge exchange lifetimes of the  $H^+$ ,  $O^+$ , and  $He^+$  ions at these energies are different enough to theoretically allow identification of different ion species by measuring the decay rates of the ions. The data shown in Figure 3 during the "decay period" were fitted to a double exponential decay function (eq. 1). The  $\alpha_i$ 's (ion fluxes) and  $\tau_i$ 's (lifetimes) were free variables and determined by the best fit to the data. The charge exchange lifetimes of  $H^+$  and  $O^+$  for the same conditions as under which the data were taken agree remarkably well to fitted lifetimes  $\tau_1$  and  $\tau_2$  in each of the three storms. For example, in the February storm  $\tau_1$  was  $3.27 \times 10^4$  sec and  $\tau_2$  was  $1.63 \times 10^5$  sec, whereas  $\tau(H^+)$  is  $3.64 \times 10^4$  sec and  $\tau(O^+)$  is  $1.78 \times 10^5$  sec. It appears, therefore, due to the close agreement of the charge exchange lifetime values with those fitted lifetime determined from the actual measurements, that one can infer the presence of significant quantities of  $O^+$  in the storm-time ring current. This occurs not just in an isolated case, but in each of the three storms we have analyzed. This inference technique was applied to the data at energies above and below the 9.2 keV channel described above as well as for L-values above and below the  $L = 4.25$  case also described above.

#### Energy and L-Value Dependence

The electrostatic analyzer on Explorer 45 has an energy range of 0.7 to 30.2 keV. For convenience and to avoid consideration of coulomb scattering effects which became more important below 1 to 2 keV we have considered four energy detector channels in the higher end of this energy range. The energy band width and center energy of these channels are given in Table 2. Figure 5 shows the measured fluxes at  $L = 4.25$  in the four energy bands,

TABLE 2: ENERGY BANDS

Center Energy (keV)	$E_{\min}$ (keV)	$E_{\max}$ (keV)
6.0	5.25	7.13
9.2	7.97	10.81
13.5	11.74	15.93
25.6	22.29	30.23

6.0, 9.2, 13.5 and 25.6 keV for the February, 1972, geomagnetic storm. The data at 9.2 keV are identical to that shown in Figure 3. The same fitting procedure as for the 9.2 keV case described earlier was employed for the other three energies. The fitted values of  $\tau_1$  and  $\tau_2$  agree well with the charge exchange lifetimes for  $H^+$  and  $O^+$ . The solid curves through the data were determined by using the predicted charge exchange lifetime values for  $H^+$  and  $O^+$  with the fitted  $\alpha_1$  and  $\alpha_2$  values and normalized to the first data point. Of course, curves derived using the fitted  $\tau_1$  and  $\tau_2$  values show even better agreement than these.

Since the Explorer 45 had an apogee slightly above  $L = 5$  (Figure 2), we have selected three L-values (5.0, 4.25 and 3.5) which span the storm time ring current region as much as possible and are equally spaced. At  $L = 5$ , due to the altitude increase, the neutral hydrogen density,  $n$ , decreased and was computed to be  $135/\text{cm}^3$  for the February storm. As described above, the data for each energy were fitted to a double exponential decay function (eq. 1) and the ion lifetimes,  $\tau_i$ 's, and quantities,  $\alpha_i$ 's were determined by the best fit to the data. A comparison between the fitted  $\tau_i$ 's and the charge exchange lifetimes of  $H^+$  and  $O^+$  for these same conditions showed remarkable agreement at  $L = 5$ . For example, at 13.5 keV  $\tau_1 = 5.70 \times 10^4$  sec and  $\tau_2 = 2.26 \times 10^5$  sec, whereas  $\tau(H^+)$  is  $5.88 \times 10^4$  sec and  $\tau(O^+)$  is  $2.31 \times 10^5$  sec.

The situation at  $L = 3.5$  is somewhat different. The measured fluxes in the four energy bands at this L-value are shown in Figure 6. As in all cases before, the data for each energy were fitted to a double exponential decay function. However, contrary to the previous cases, the chi-square of the fits were not nearly as good as before. For the 6.0 keV and 9.2 keV cases it was found that better fits, based on chi-squared,

were obtained if the first data point (from February 24, 1972) was not included in the double exponential decay fit. The  $\tau_1$  and  $\tau_2$  values for 9.2 keV were found to be  $9.34 \times 10^4$  sec and  $7.90 \times 10^5$  sec which are in close agreement to the  $O^+$  and  $He^+$  lifetimes of  $1.09 \times 10^5$  sec and  $6.49 \times 10^5$  sec, respectively. The situation is interpreted that the  $H^+$  decay at  $L = 3.5$  during the first 8 hours was substantial and thereafter only  $O^+$  and  $He^+$  existed in "observable" quantities. As can be seen in Figure 4 at 6.0 keV and at  $L = 3.5$  the drop in the normalized flux for  $H^+$  during the first 8 hours under charge exchange decay is from 1.0 to 0.25, quite a substantial drop.

The manner in which the above double exponential decay curves for 6.0 and 9.2 keV deviated from the measured fluxes lead us to consider using a triple exponential decay function of the form

$$f = \alpha_1 e^{-(t/\tau_1)} + \alpha_2 e^{-(t/\tau_2)} + \alpha_3 e^{-(t/\tau_3)} \quad (2)$$

This implies that there could be three ions present in measurable quantities (if  $\alpha_3 \neq 0$ ) with the  $\tau_i$ 's sufficiently different from each other that the fitting procedure is sensitive to the difference. Amazingly, for 25.6 keV the fitted value of  $\tau_3$ ,  $2.14 \times 10^5$  sec, is very close to the predicted charge exchange lifetime value  $He^+$  ions would have,  $\tau(He^+) = 2.40 \times 10^5$  sec, at this L-value and geophysical conditions where the neutral hydrogen density,  $n$ , is  $403/cm^3$ . The other two lifetimes,  $\tau_1$  and  $\tau_2$ , were comparable to the charge exchange lifetime of  $H^+$  and  $O^+$ , respectively. A triple exponential decay was also used for the data at 13.5 keV and also yielded lifetimes close to the charge exchange decay lifetimes of  $H^+$ ,  $O^+$ , and  $He^+$ . Apparently, with the higher neutral hydrogen density

at this lower L-value the lifetimes of  $H^+$  and  $O^+$  are short enough such that they decay from their enhanced intensity to a level at which the  $He^+$  intensity becomes "observable" through this technique.

#### Mirror Latitude Dependence

Thus far we have presented the Explorer 45 measurements of those particles which mirror near the geomagnetic equator. The relationship between the charge exchange lifetimes of particles mirroring off the geomagnetic equator to the lifetime of particles confined to the equator is  $\tau_m = \tau_e \cos^j \lambda_m$ , where  $j = 3.5 \pm 0.2$  (Smith and Bewtra, 1976). For this February, 1972, magnetic storm at the L-values we are considering, Smith and Bewtra (1976) showed that the cosine dependence is more precisely given by  $\cos^{3.4} \lambda_m$ . For  $\lambda_m = 14^\circ$  the lifetimes,  $\tau_m$ , are reduced by only 10% from the equatorial values. However, for  $\lambda_m = 35^\circ$ , for example, the lifetimes are shortened by nearly a factor of 2 from the equatorial values. The equatorial pitch angle for particles mirroring at  $35^\circ$  is about  $28^\circ$ .

Figure 7 shows the measured ion fluxes at  $\lambda_m = 35^\circ$  for the 9.2 keV energy channel at  $L = 4.25$ . A triple exponential decay function (eq. 2) was used to fit the data. The fitted values of  $\tau_1$ ,  $\tau_2$ , and  $\tau_3$  are  $2.81 \times 10^4$  sec,  $1.25 \times 10^5$  sec and  $5.69 \times 10^5$  sec, respectively. These values are to be compared to the  $H^+$ ,  $O^+$  and  $He^+$  charge exchange lifetimes, which are,  $2.05 \times 10^4$  sec,  $1.13 \times 10^5$  sec and  $6.69 \times 10^5$  sec, respectively. The solid curve in Figure 7 is determined by using the predicted charge exchange lifetime values for the three ions and the fitted values for the ion quantities,  $\alpha_i$ 's. If the fitted  $\tau_i$ 's were used the solid curve would again be in better agreement.

To show graphically the inferred contribution of  $\text{He}^+$  at these low equatorial pitch angles, the expected flux level of the combination of  $\text{H}^+$  and  $\text{O}^+$  is shown as a dashed curve in Figure 7. This curve was determined by using the fitted  $\alpha_1$  and  $\alpha_2$  values, and the  $\tau(\text{H}^+)$  and  $\tau(\text{O}^+)$  values. This shows that  $\text{H}^+$  and  $\text{O}^+$  can not be the only two ions being measured.

## OXYGEN AND HELIUM IONS IN RING CURRENT

The results of our analyses of the February 24, 1972, geomagnetic storm clearly infer that not only are oxygen ions abundant in the storm-time ring current, but helium ions are also "observable". The helium ions in the energy range we are considering are most obvious at the lower altitude. We saw this for the ions at  $L = 3.5$ , the lowest  $L$ -value we considered as well as for the ions which were mirroring quite well down the field line ( $\lambda_m = 35^\circ$ ). This is principally due to the fact that the charge exchange lifetimes are shorter for ions flowing through a larger density of neutral hydrogen such as occurs at the lower  $L$ -values and lower mirror latitudes, and the fitting technique for two or three ions is more sensitive to the shorter lifetimes since we have a limited number of measurements during a finite decay period (Figure 3).

One is now confronted by the possibility that the double exponential decay fits, as good as they are at  $L = 4.25$  and  $L = 5.0$ , do not yield the full informational content of the data. Therefore, we have fitted the triple exponential decay function to the data to provide consistency in our approach, realizing that the helium ions may be negligible in some of the cases. The three ion fit was applied to the February and May data (Figure 3) at  $L = 4.25$  and for an energy of 9.2 keV. We attempted to fit the December 17, 1971 storm at the same  $L$ -value and energy, but the "decay period" was too short to get a meaningful fit with the third ion. A minimum of three days is needed to get  $\text{He}^+$  fits under these conditions. The fitted  $\tau_i$ 's and  $\alpha_i$ 's were used to determine the solid curves through the data in Figure 3 and are given in Table 3 for the

three storms. The lifetimes are also given for  $H^+$ ,  $O^+$  and  $He^+$  at this energy and for the appropriate geophysical conditions given in Table 1. In all three storms the fitted  $\tau_i$ 's agree well with the  $H^+$ ,  $O^+$  and  $He^+$  lifetimes. The  $\tau_1$  values generally are larger than the predicted values for  $H^+$  and this difference will be addressed below in reference to a possible  $He^{++}$  contribution. The other remarkable result, beside the agreement with the three ion species, is the general consistency of the fitted  $\tau_i$ 's for the three storms.

The  $\alpha_i$  values represent the intensity of each of the ion species at  $t = 0$ , the time associated with the beginning of the fitting. This is approximately the beginning of the "decay period" as shown in Figure 3. The  $t = 0$  point for the February and May storms is slightly delayed from the main phase maximum point. In the December storm, however, the  $t = 0$  point is significantly shifted with respect to the main phase maximum. The values of  $\alpha_1$ ,  $\alpha_2$  and  $\alpha_3$  for February and May are quite comparable for the two storms and are approximately in the same proportions. In the December storm  $\alpha_1$  is smaller than  $\alpha_2$ . This inversion of the relative quantities could be due to the fact that only a double exponential decay function was used in the fit, but it does not seem very likely. Instead what we may have observed is the charge exchange decay of  $H^+$  ions ( $\alpha_1$ ) before our  $t = 0$  start to a level below  $O^+$  ions ( $\alpha_2$ ). This would have occurred during the "storm-related activity" period in Figure 3. The values of  $\alpha_3$ , corresponding to  $He^+$  ions, are quite small at  $t = 0$  compared to  $\alpha_1$  and  $\alpha_2$ .

The data at  $L = 5$  are presented in Figure 8 for completeness of the data set for the February storm and the data are in the same format and

TABLE 3: ION LIFETIMES AND INTENSITIES (L = 4.25; E = 9.2 keV)\*

	Dec 17, 1971	Feb 24, 1972	May 15, 1972
Fitted Lifetime $\tau_1$	$4.04 \times 10^4$ sec	$4.34 \times 10^4$ sec	$4.22 \times 10^4$ sec
Predicted Lifetime $H^+$	$3.91 \times 10^4$ sec	$3.64 \times 10^4$ sec	$3.93 \times 10^4$ sec
Fitted Lifetime $\tau_2$	$2.00 \times 10^5$ sec	$2.32 \times 10^5$ sec	$2.17 \times 10^5$ sec
Predicted Lifetime $O^+$	$2.16 \times 10^5$ sec	$2.01 \times 10^5$ sec	$2.17 \times 10^5$ sec
Fitted Lifetime $\tau_3$	---	$1.10 \times 10^6$ sec	$1.10 \times 10^6$ sec
Predicted Lifetime $He^+$	$1.28 \times 10^6$ sec	$1.19 \times 10^6$ sec	$1.29 \times 10^6$ sec
$\alpha_1$ ( $cm^2$ sec sr keV) $^{-1}$	$1.39 \times 10^6$	$1.85 \times 10^6$	$2.04 \times 10^6$
$\alpha_2$ ( $cm^2$ sec sr keV) $^{-1}$	$2.06 \times 10^6$	$1.28 \times 10^6$	$1.06 \times 10^6$
$\alpha_3$ ( $cm^2$ sec sr keV) $^{-1}$	---	$5.12 \times 10^4$	$5.06 \times 10^4$

\* For  $\lambda_m = 14^\circ$

with the same selection criteria for the data at  $L = 4.25$  (Figure 5) and  $L = 3.5$  (Figure 6). The solid curves, however, are the results of the triple exponential decay functional fits and are determined by using the predicted charge exchange lifetimes values for  $H^+$ ,  $O^+$  and  $He^+$  together with the fitted values for  $\alpha_1$ ,  $\alpha_2$  and  $\alpha_3$  as was done in the previous cases. These curves show excellent agreement with the data.

Up to this point we have presented the fitted lifetimes in comparison with the predicted charge exchange decay lifetimes on a case by case basis, i.e., for each given energy and L-value. In order that one gets a clearer understanding of the relative correspondence of the fitted  $\tau_i$ 's to the predicted values, the fitted  $\tau_i$ 's determined by the triple exponential decay functions are shown as a function of energy in Figures 9a-c for the three L-values, 3.5, 4.25 and 5.0, respectively. The solid curves from 1 to 100 keV are the predicted charge exchange decay lifetimes for the February 1972 geomagnetic storm for ions mirroring at  $\lambda_{\text{m}} = 14^\circ$ . The fitted lifetimes at the four energies, 6.0, 9.2, 13.5 and 25.6 keV, cluster about the predicted lifetimes of  $H^+$ ,  $O^+$  and  $He^+$  for each of the three L-values. The fitted lifetimes corresponding to  $O^+$  and  $He^+$  ions are well ordered in energy, show excellent agreement with the predicted lifetime values and are well separated from each of the other two ions. The one value for these two ions with the largest deviation from the predicted value is in the 13.5 keV energy band at  $L = 5.0$ . We have analyzed these data and can find no apparent reason outside possible substorm injection effects for the deviation, which is not all that large except in comparison with the excellent agreement at all the other values.

As was mentioned earlier the  $H^+$  and  $He^{++}$  charge exchange lifetimes

(with the energy of the  $\text{He}^{++}$  shifted a factor of two) are close to one another and are overlapping at about 11 keV. The  $\text{He}^{++}$  charge exchange lifetimes are shown also in Figure 9a-c, but with the energy scale shifted by a factor of two to reflect the energy bands in the electrostatic analyzer in which the  $\text{He}^{++}$  ions would be measured. The results in general for  $\tau_1$  show overall consistency with  $\text{H}^+$  especially if the  $\text{He}^{++}$  curve is ignored. In examining this more closely, however, one is drawn to the value at 25.6 keV which is nearly in the middle of the  $\text{H}^+$  and  $\text{He}^{++}$  curves especially at the two lower L-values. At  $L = 5$  it is between the two curves but closer to the  $\text{H}^+$  curve. In addition, the value of  $\tau_1$  at 6.0 keV is also between the two curves. This strongly suggests a mixture of  $\text{H}^+$  and  $\text{He}^{++}$  ions. Due to the relative closeness in the predicted lifetimes the fitting technique by itself could not resolve  $\text{He}^{++}$  from  $\text{H}^+$ , as we were able to do with  $\text{O}^+$  and  $\text{He}^+$ . The general trend of the fitted  $\tau_1$ 's, considering the three L-values together suggest that at  $L = 5$  the agreement is much closer to  $\text{H}^+$  and at  $L = 3.5$  the trend has shifted toward a better agreement with  $\text{He}^{++}$ . Recall also, that for the  $\text{He}^{++}$  ions the energy of the measured ions (if any) is twice the energy of the detector center energy. Thus any mixture of  $\text{H}^+$  and  $\text{He}^{++}$  which may be present are really mixtures at two different energies (e.g. 25.6 keV for  $\text{H}^+$  and 51.2 keV for  $\text{He}^{++}$ ). One can therefore consider that the  $\text{He}^{++}$  may be more abundant at the higher energies than it is at the lower energies.

### Conclusions

Through the application of the inference technique which we have described in this paper, it is possible that the ion composition of the

ring current in the energy range of an electrostatic analyzer can be inferred for moderate to large geomagnetic storms. Using this method we infer that oxygen ions in the range 5 to 30 keV are quite abundant in the storm time ring current and that in the recovery phase, one or two days after the main phase maximum,  $O^+$  ions can have intensities greater than  $H^+$  ions. We also infer that  $He^+$  can be found in "measurable" quantities at these energies and L-values but that the intensities of  $He^+$  ions are much smaller than those for  $H^+$  and  $O^+$ . However, as the recovery phase continues the  $H^+$  ions, which are removed rapidly by charge exchange decay, become small in intensity, and the  $O^+$  ions after several days are reduced to intensities comparable to the  $He^+$  intensities.

It thus appears that the  $He^+$  ions may form most of what we consider to be the quiet-time ring current, and it is the hydrogen ions which are the subject of the initial storm injection and most assuredly are associated with substorm injections.

Additionally, the possibility that  $He^{++}$  could also be present in the ring current is evident in our summary results. While the nature of this identification is not nearly as strong as our inference of  $O^+$  and  $He^+$ , it presents a distinct possibility.

These results make one realize that infrequent measurements through the ring current, with say an ion mass spectrometer, will not sufficiently identify the ion composition since the mixture of ions is constantly changing due to their decay properties and due to the repeated injection of fresh particles into this region. It would, however, give a definitive "snapshot" of the ion composition which could be analyzed in terms of the scenario we have presented in this paper.

## SUMMARY

The analysis of data from the Explorer 45 (S<sup>3</sup>-A) electrostatic analyzer in the energy range 5 to 30 keV has provided some new results on the ring current ion composition. By analyzing the measured decay rates of the ions after geomagnetic storms and assuming two or more ions were present and that the decays were exponential in nature we were able to establish three separate lifetimes for the ions. By using the recently revised charge exchange decay lifetimes (Smith and Bewtra, 1977) and the dependence of these lifetimes on the mirror latitudes of these particles we determined for three geomagnetic storms the expected charge exchange lifetimes for H<sup>+</sup>, O<sup>+</sup> and He<sup>+</sup> in the energy and L-value range of the data. In this paper we showed the close agreement of the fitted decay lifetimes from the measurements to the charge exchange decay lifetimes to these three ions and inferred that H<sup>+</sup>, O<sup>+</sup> and He<sup>+</sup> existed in the storm-time ring currents we considered. We also found indication that He<sup>++</sup> may also be present. The agreement is consistent in energy (5 to 30 keV), L-value (3.5 to 5.0), at least two widely spaced mirror latitudes ( $\lambda_m = 14^\circ$  and  $35^\circ$ ) and for three geomagnetic storms. We have thus developed an inference technique to measure the ion composition in the ring current using an electrostatic analyzer.

## REFERENCES

- Allen, J. H., C. C. Abston, and L. D. Morris, Auroral electrojet magnetic activity indices, AE(11), for 1972, World Data Center A Report UAG-45, 1975.
- Berko, F. W., L. J. Cahill, Jr., and T. A. Fritz, Protons as prime contributors to the storm-time ring current, J. Geophys. Res., 80, 3549-3552, 1975.
- Cahill, L. J., Jr., Magnetic storm inflation in the evening sector, J. Geophys. Res., 78, 4724-4730, 1973.
- Cahill, L. J., Jr., and Y. C. Lee, Development of four small magnetic storms in February, 1972, Planet. Space Sci., 23, 1279-1292, 1975.
- Cornwall, J. M., F. V. Coroniti, and R. M. Thorne, Turbulent loss of ring current protons, J. Geophys. Res., 75, 4699-4709, 1970.
- Cowley, C. W. H., Pitch angle dependence of the charge-exchange lifetime of ring current ions, Planet. Space Sci., 25, 385-393, 1977.
- Dressler, A. J., and E. N. Parker, Hydromagnetic theory of geomagnetic storms, J. Geophys. Res., 64, 2239, 1959.
- Frank, L. A., On the extraterrestrial ring current during geomagnetic storms, J. Geophys. Res., 72, 3753-3767, 1967.
- Frank, L. A., K. L. Ackerson, and D. M. Yeager, Observations of atomic oxygen ( $O^+$ ) in the earth's magnetotail, J. Geophys. Res., 82, 129-134, 1977.
- Johnson, R. G., R. D. Sharp, and E. G. Shelley, Observations of ions of ionospheric origin in the storm-time ring current, Geophys. Res. Letters, 4, 403-406, 1977.
- Liemohn, H., The lifetimes of radiation belt protons with energies between 1 keV and 1 MeV, J. Geophys. Res., 66, 3593-3595, 1961.
- Lyons, L. R., and D. S. Evans, The inconsistency between proton charge exchange and the observed ring current decay, J. Geophys. Res., 81, 6197-6200, 1976.
- McClure, G. W., Electron transfer in proton-hydrogen-atom collisions: 2-117 keV, Phys. Rev., 148, 47-54, 1966.
- McIlwain, C. E., Ionospheric ions at 6.6 earth radii, in EOS, 58, 1212, 1977.
- Prolss, G. W., Decay of the magnetic storm ring current by the charge-exchange mechanism, Planet. Space Sci., 21, 983-992, 1973.

- Sharp, R. D., R. G. Johnson, and E. G. Shelley, The morphology of energetic  $O^+$  ions during two magnetic storms: Temporal variations, J. Geophys. Res., 81, 3283-3291, 1976a.
- Sharp, R. D., R. G. Johnson, and E. G. Shelley, The morphology of energetic  $O^+$  ions during two magnetic storms: Latitudinal variations, J. Geophys. Res., 81, 3292-3298, 1976b.
- Shelley, E. G., R. G. Johnson, and R. D. Sharp, Satellite observations of energetic heavy ions during a geomagnetic storm, J. Geophys. Res., 77, 6104-6110, 1972.
- Shelley, E. G., R. D. Sharp, and R. G. Johnson, Satellite observations of an ionospheric acceleration mechanism, Geophys. Res. Letters, 3, 654-656, 1976.
- Smith, P. H., and N. K. Bewtra, Dependence of the charge exchange lifetimes on mirror latitude, Geophys. Res. Letters, 3, 689-692, 1976.
- Smith, P. H., and N. K. Bewtra, Charge exchange lifetimes for ions in the magnetosphere, (GSFC Preprint X-620-77-209), 1977, submitted for publication.
- Smith, P. H., R. A. Hoffman, and T. A. Fritz, Ring current proton decay by charge exchange, J. Geophys. Res., 81, 2701-2708, 1976.
- Swisher, R. L., and L. A. Frank, Lifetimes for low-energy protons in the outer radiation zone, J. Geophys. Res., 73, 5665-5672, 1968.
- Tinsley, B. A., Evidence that the recovery phase ring current consists of helium ions, J. Geophys. Res., 81, 6193-6196, 1976.

## FIGURE CAPTIONS

- Figure 1. Dst ( $\gamma$ ) and the AE Index ( $\gamma$ ) for six day periods covering three geomagnetic storms: December 17, 1971, February 24, 1972, and May 15, 1972.
- Figure 2. Trajectories of the Explorer 45 (S<sup>3</sup>-A) satellite orbit in L versus MLT coordinates during the three geomagnetic storms. The trajectories are for the near-equatorial orbits during these periods. The data presented in this paper were taken during the outbound portion of the orbits.
- Figure 3. Ion fluxes measured by the Explorer 45 electrostatic analyzer at L = 4.25 with an energy of 9.2 keV for the three geomagnetic storms. The fluxes were of ions mirroring at the geomagnetic latitude of 14°. This corresponds to an equatorial pitch angle of 61.3°. The sudden commencements (SC) and the times of the main phase maximum (MPM) are indicated. The solid curves through the data points are explained later in the text.
- Figure 4. Normalized flux decay expected for the ions H<sup>+</sup>, O<sup>+</sup>, He<sup>+</sup> and He<sup>++</sup> for four energies (6.0, 9.2, 13.5 and 25.6 keV) at three L-values (3.5, 4.25, 5.0) assuming only charge exchange decay mechanism of ions mirroring at  $\lambda_m = 14^\circ$  and using the February 24, 1972 magnetic storm conditions to determine the neutral hydrogen density. The He<sup>++</sup> decay curves are for ions at twice the energy indicated.
- Figure 5. Ion fluxes measured by the Explorer 45 electrostatic analyzer at L = 4.25 in four energy channels (6.0, 9.2, 13.5 and 25.6 keV). The fluxes were of ions mirroring at the geomagnetic latitude of 14°. The solid curves, described in detail in the text, were determined by assuming that the data represents a mixture of particle flux of two ions.
- Figure 6. Same as Figure 5 except now for L = 3.5. The solid curves, described in detail in the text, were determined for 6.0 and 9.2 keV by assuming that the data represents a mixture of particle flux of two ions. The curves through the 13.5 and 25.6 keV data are determined by assuming a mixture of three ions.
- Figure 7. Ion fluxes at L = 4.25 but for those 9.2 keV-particles mirroring at  $\lambda_m = 35^\circ$ . The solid curve was determined by assuming a mixture of three ions and is described in the text. The dashed curve is the normalized charge exchange decay curve under the stated conditions for a combination of H<sup>+</sup> and O<sup>+</sup> ions.

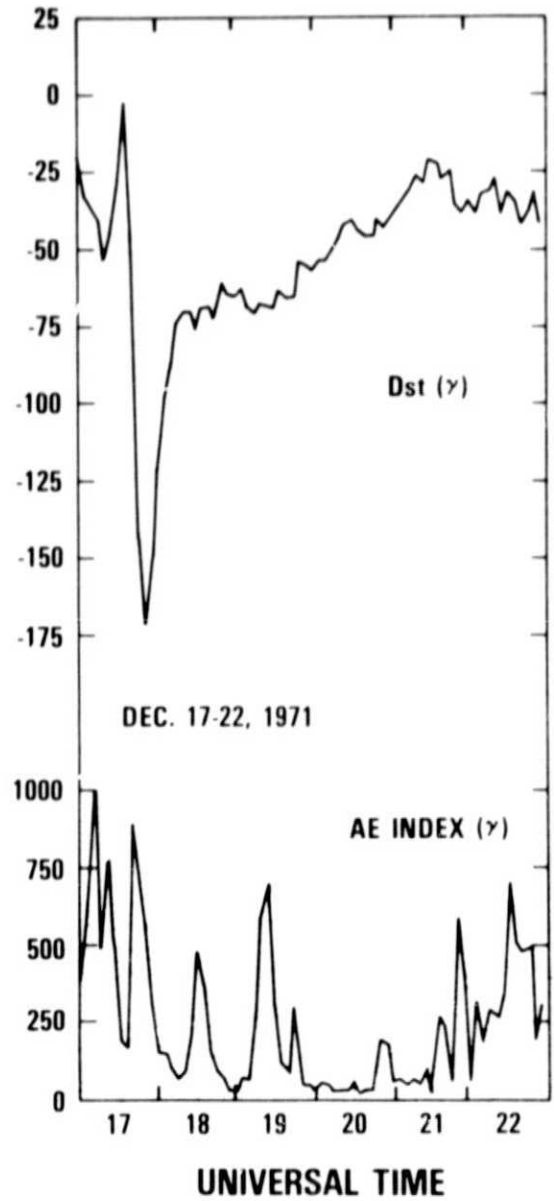
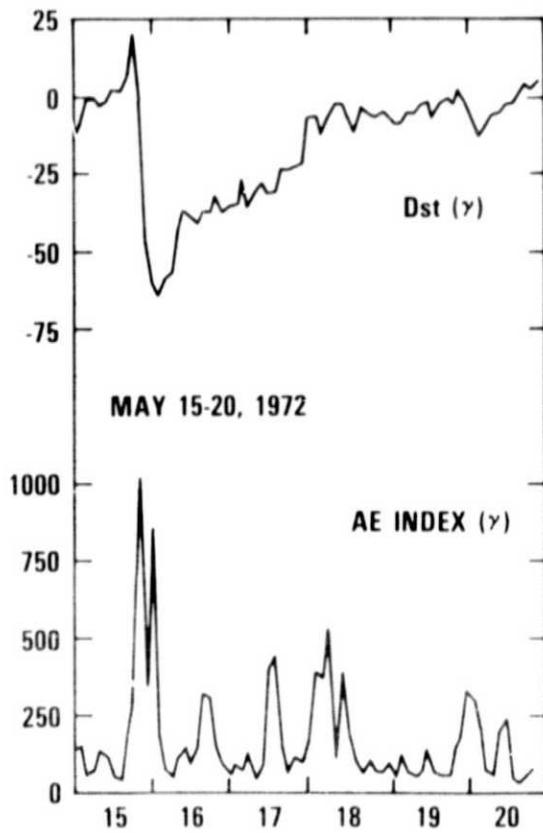
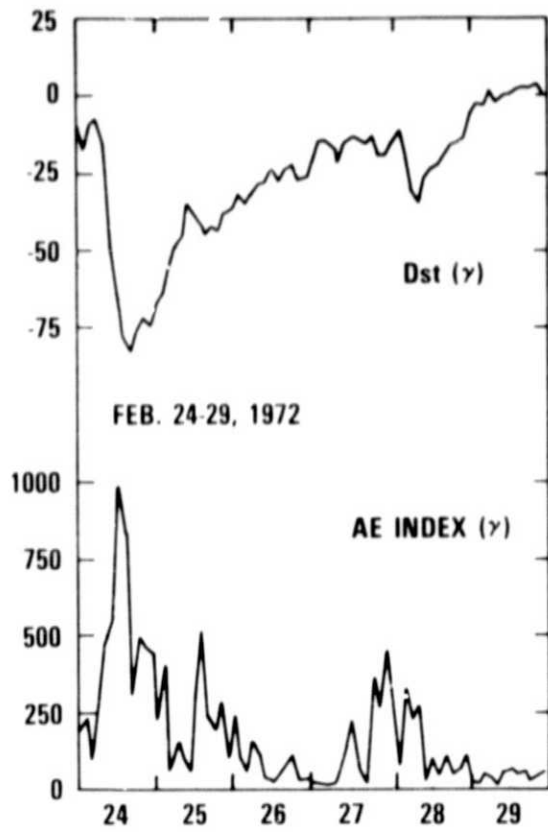


FIGURE 1

# EXPLORER 45 NEAR-EQUATORIAL ORBITS

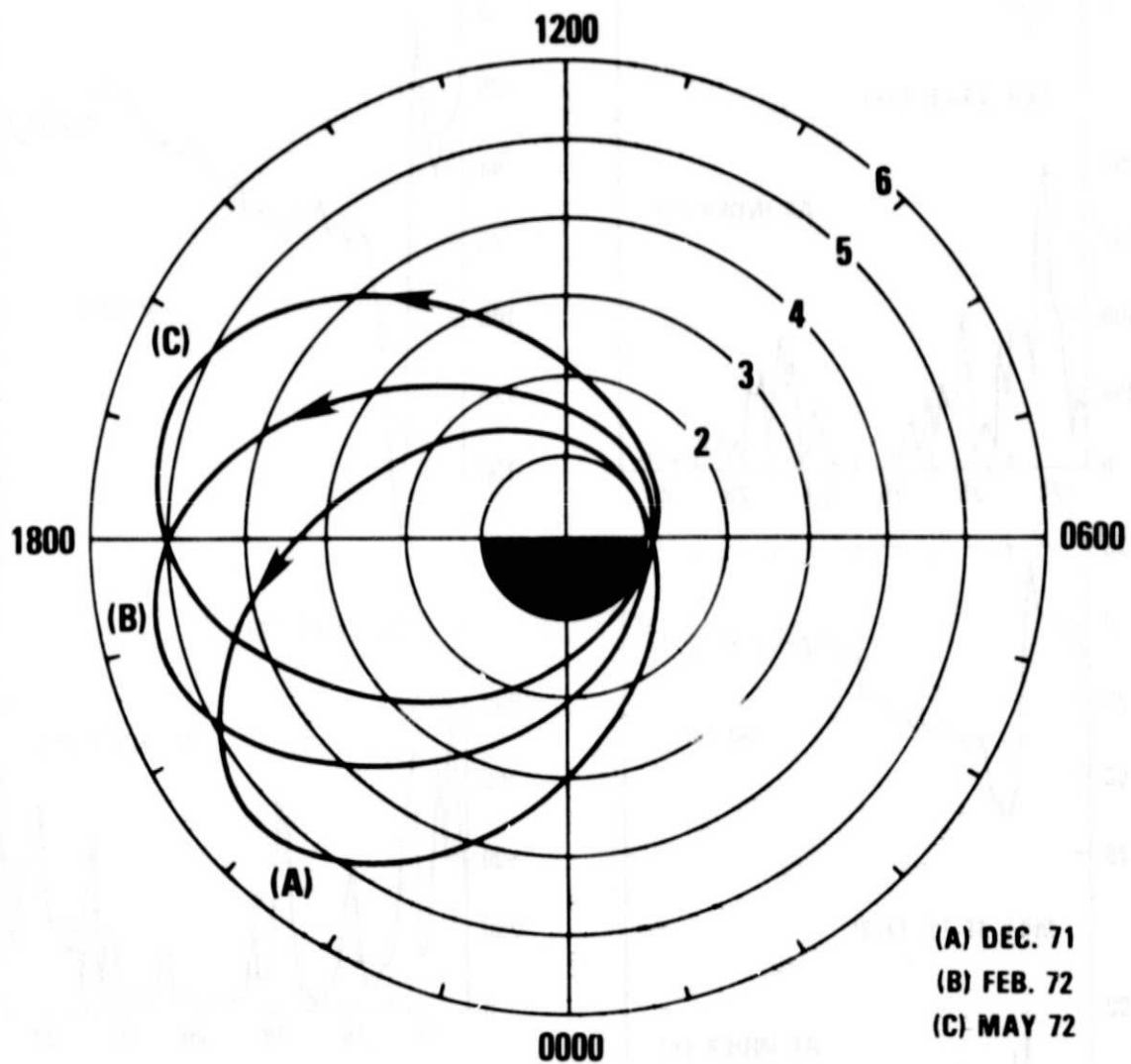


FIGURE 2

### EXPLORER 45 (S<sup>3</sup> - A)

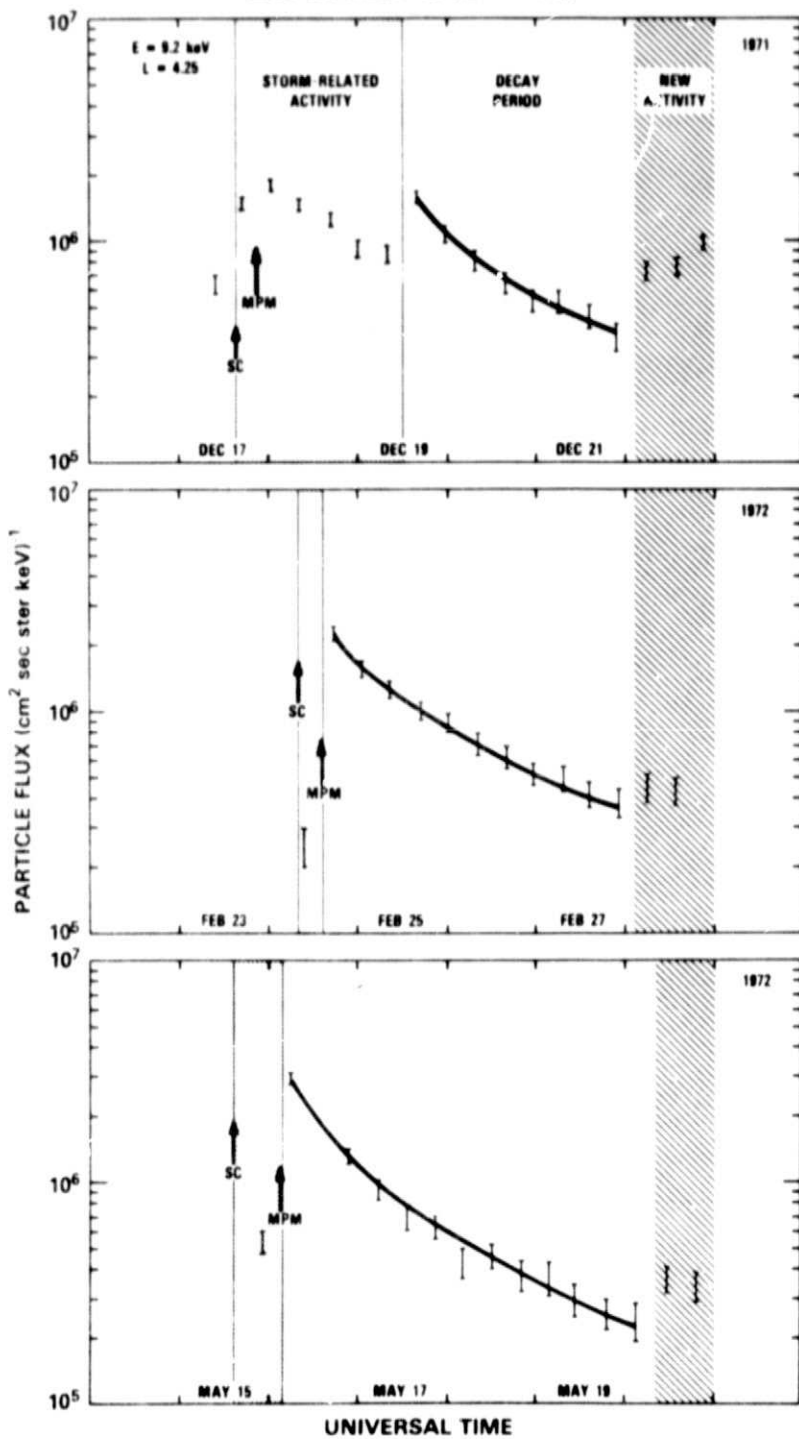


FIGURE 3

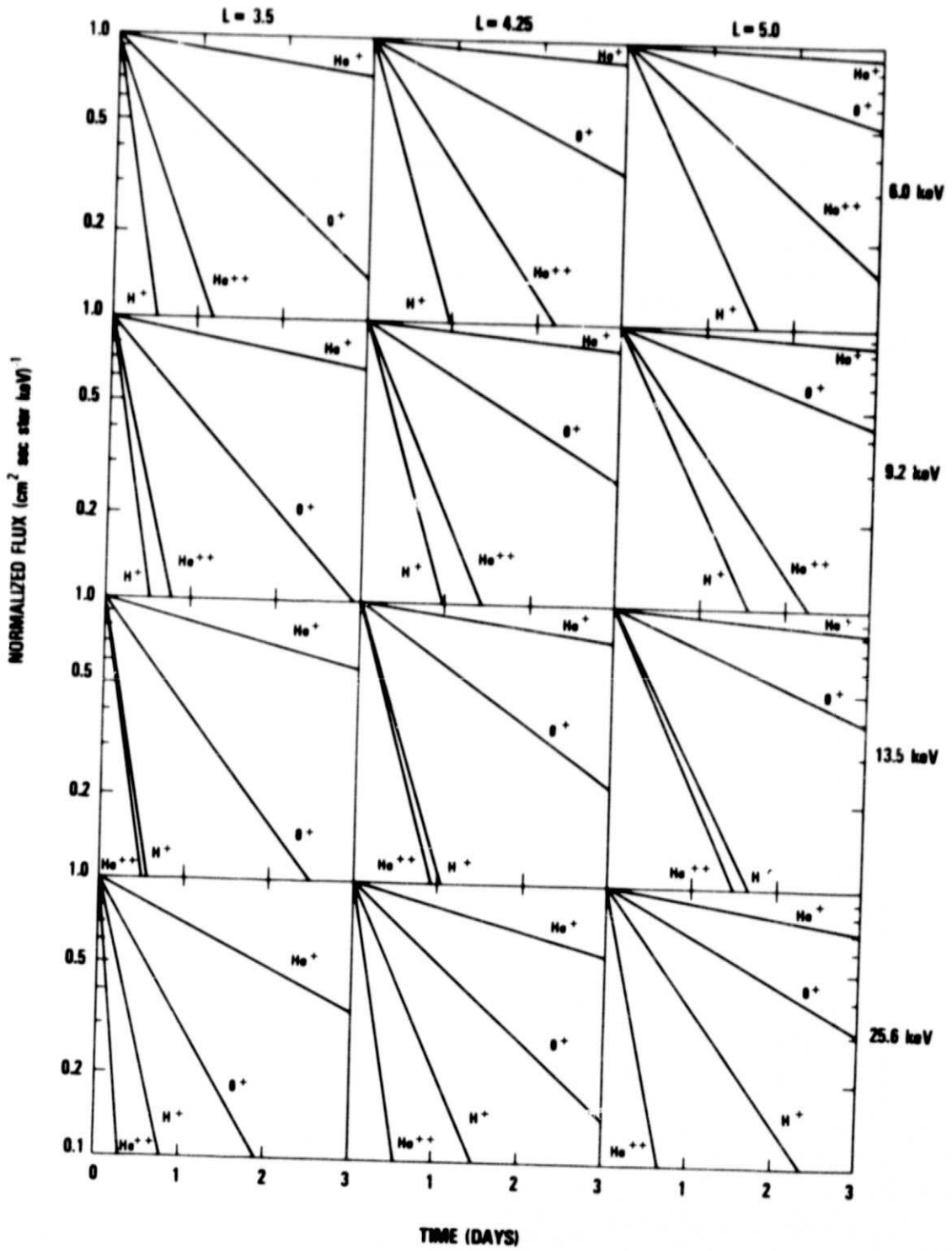


FIGURE 4

EXPLORER 45 (S<sup>3</sup>-A)

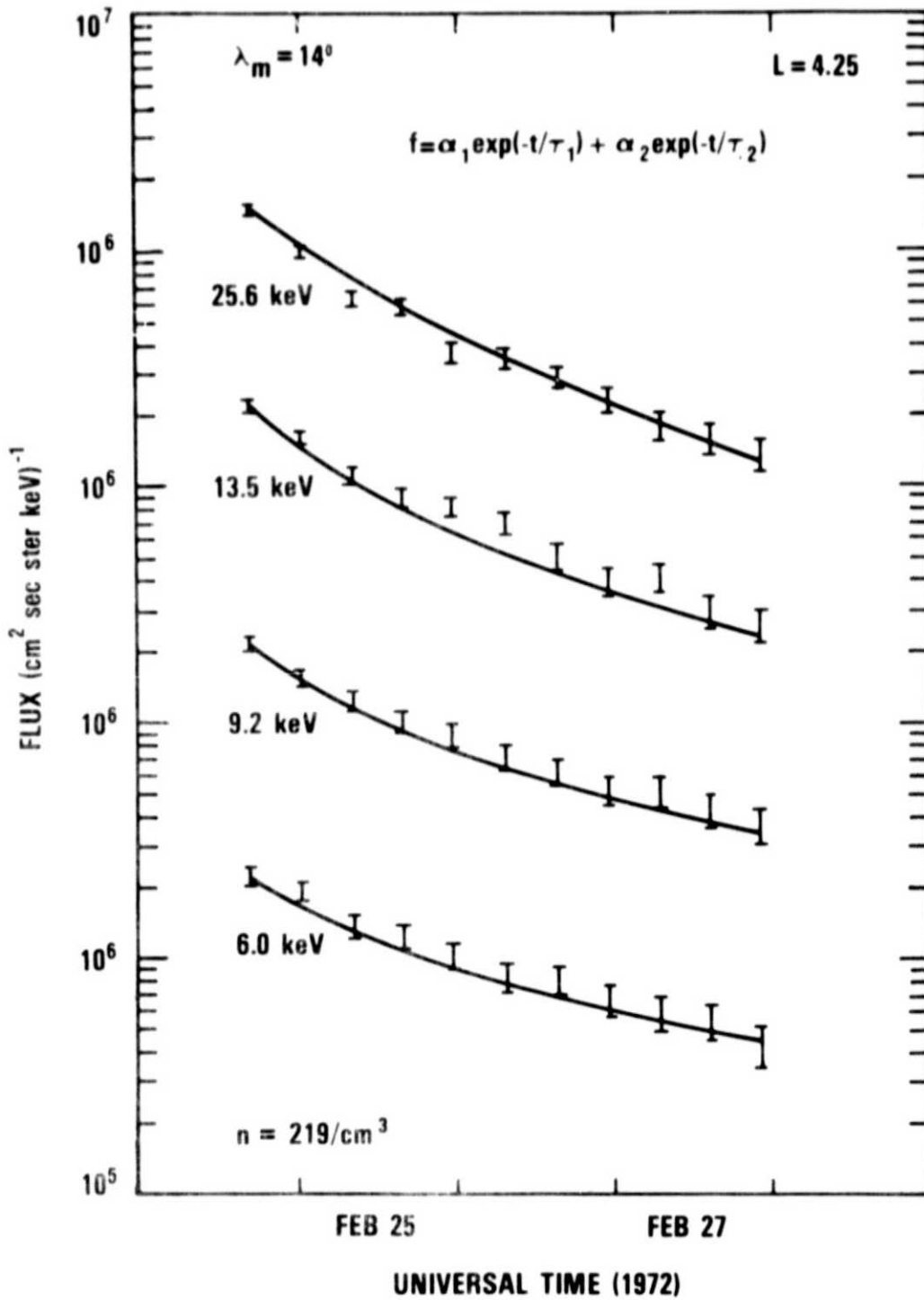


FIGURE 5

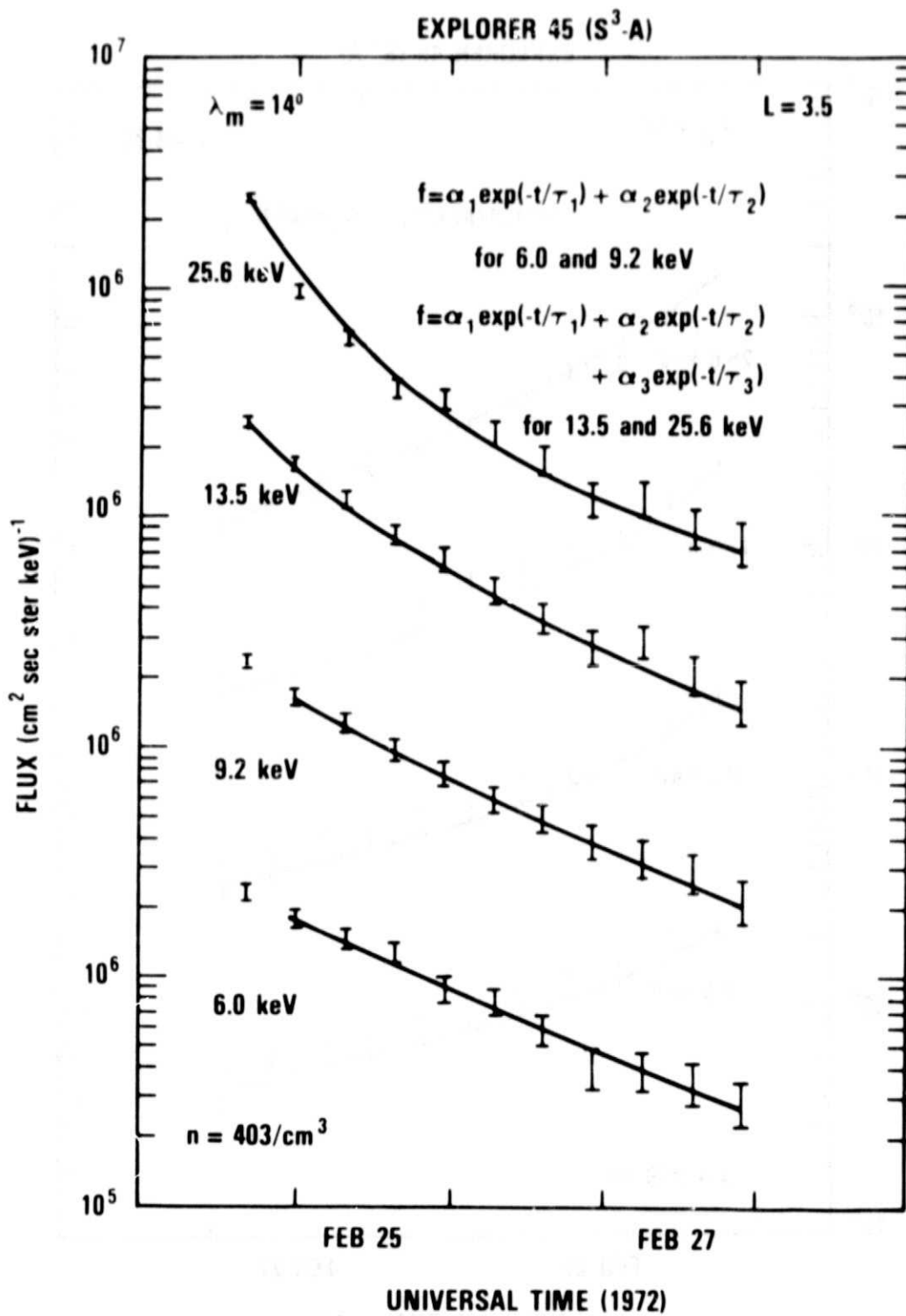


FIGURE 6

EXPLORER 45 (S<sup>3</sup>-A)

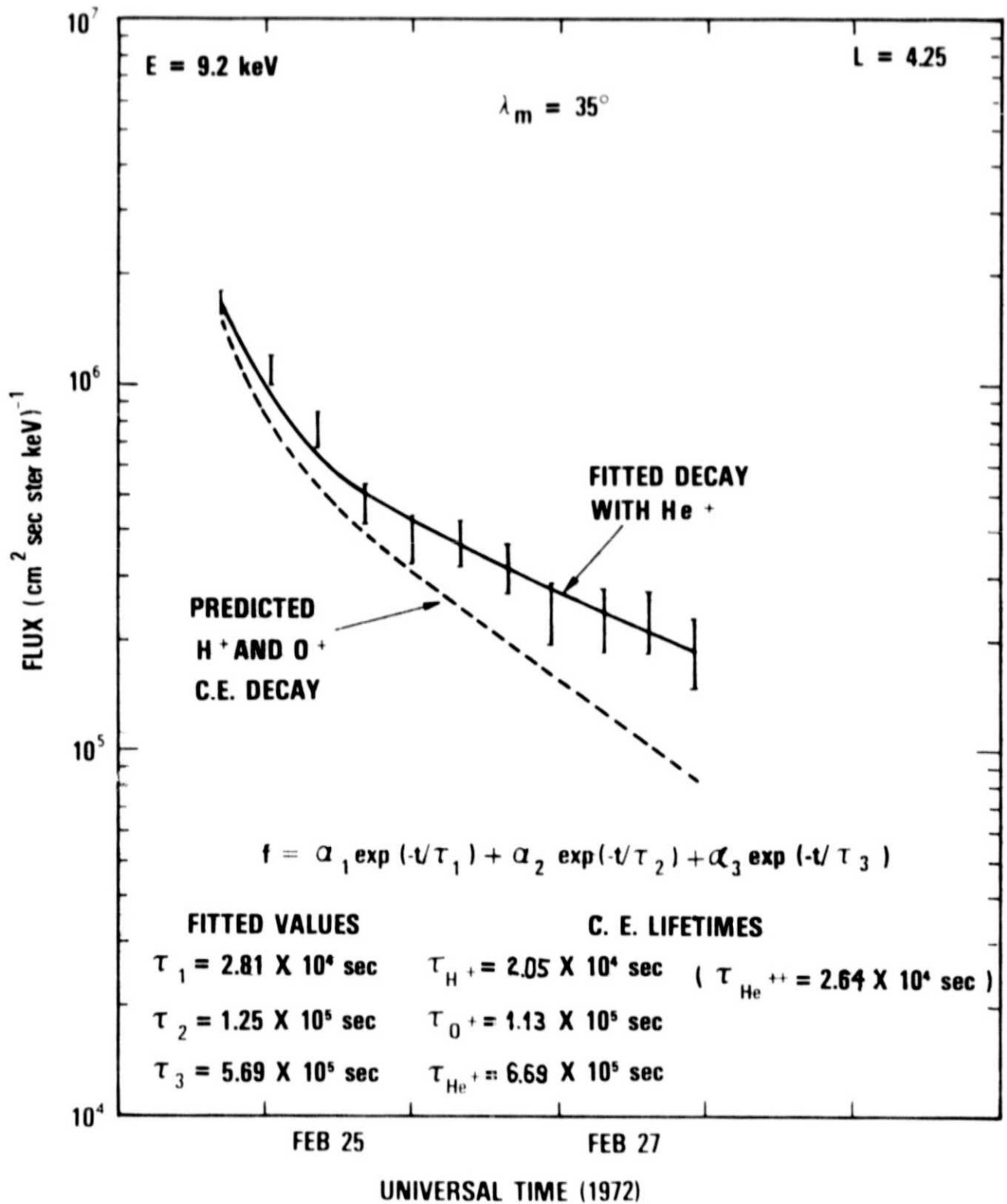


FIGURE 7

EXPLORER 45 (S<sup>3</sup>-A)

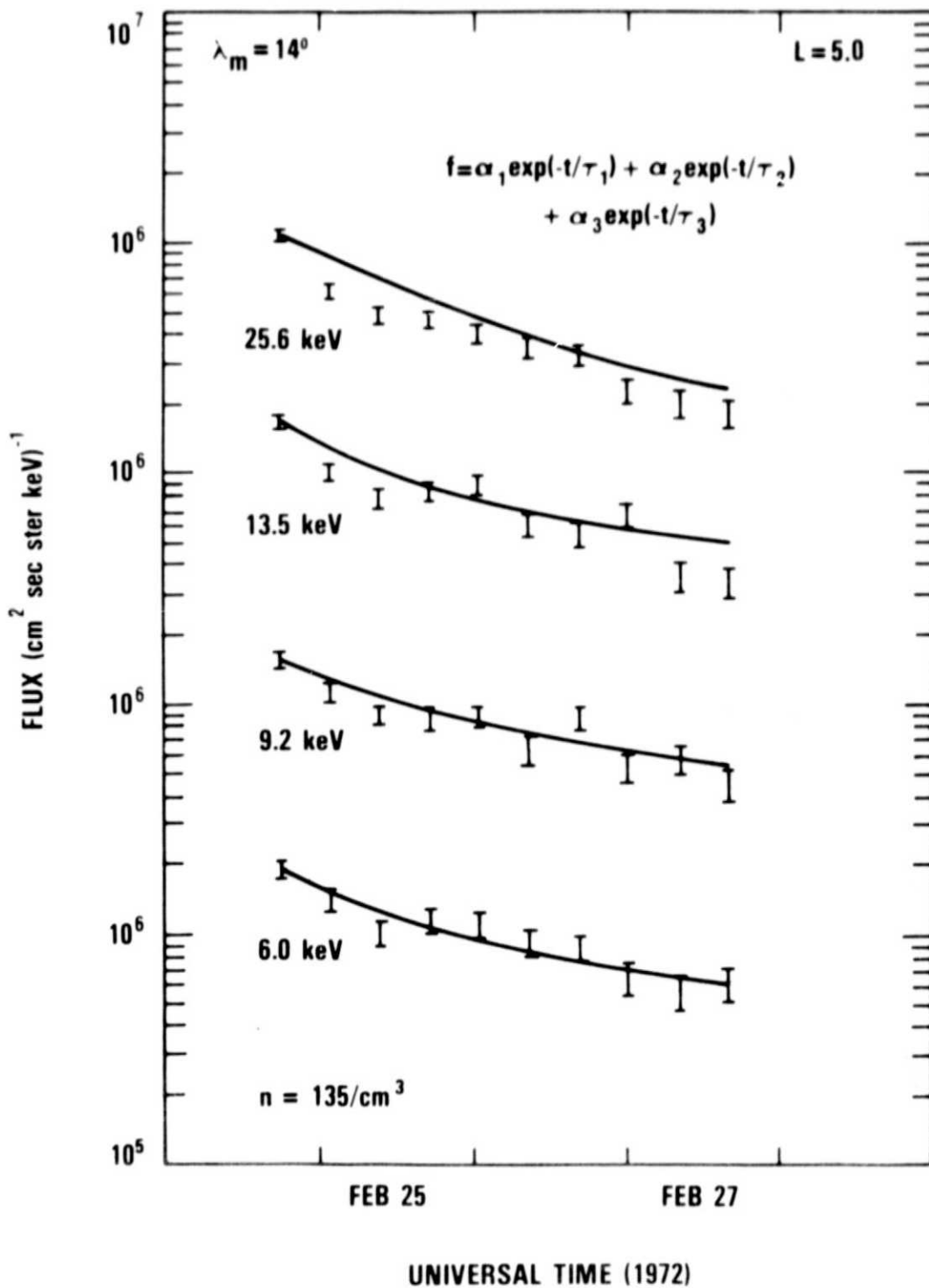


FIGURE 8

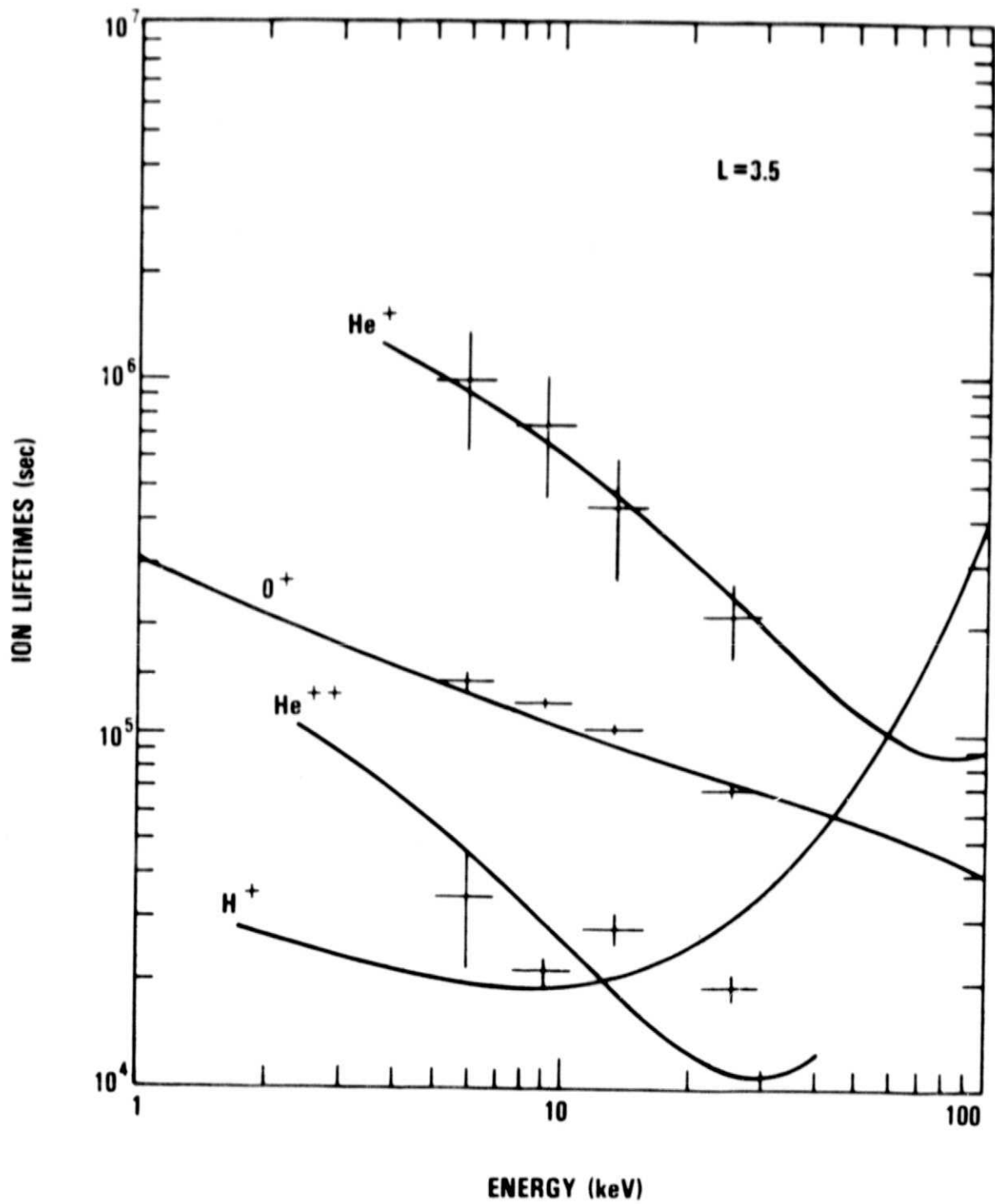


FIGURE 9a

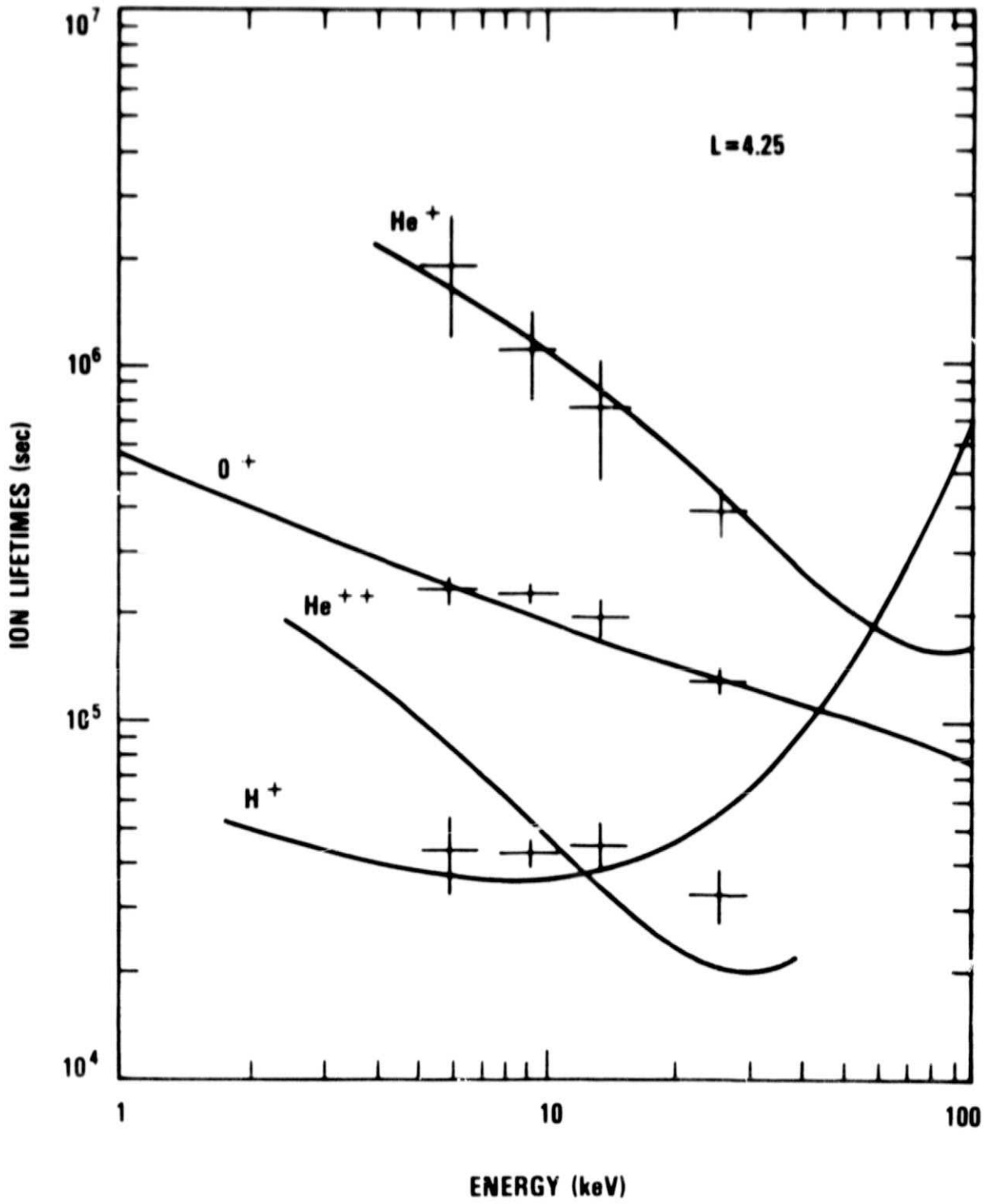


FIGURE 9b

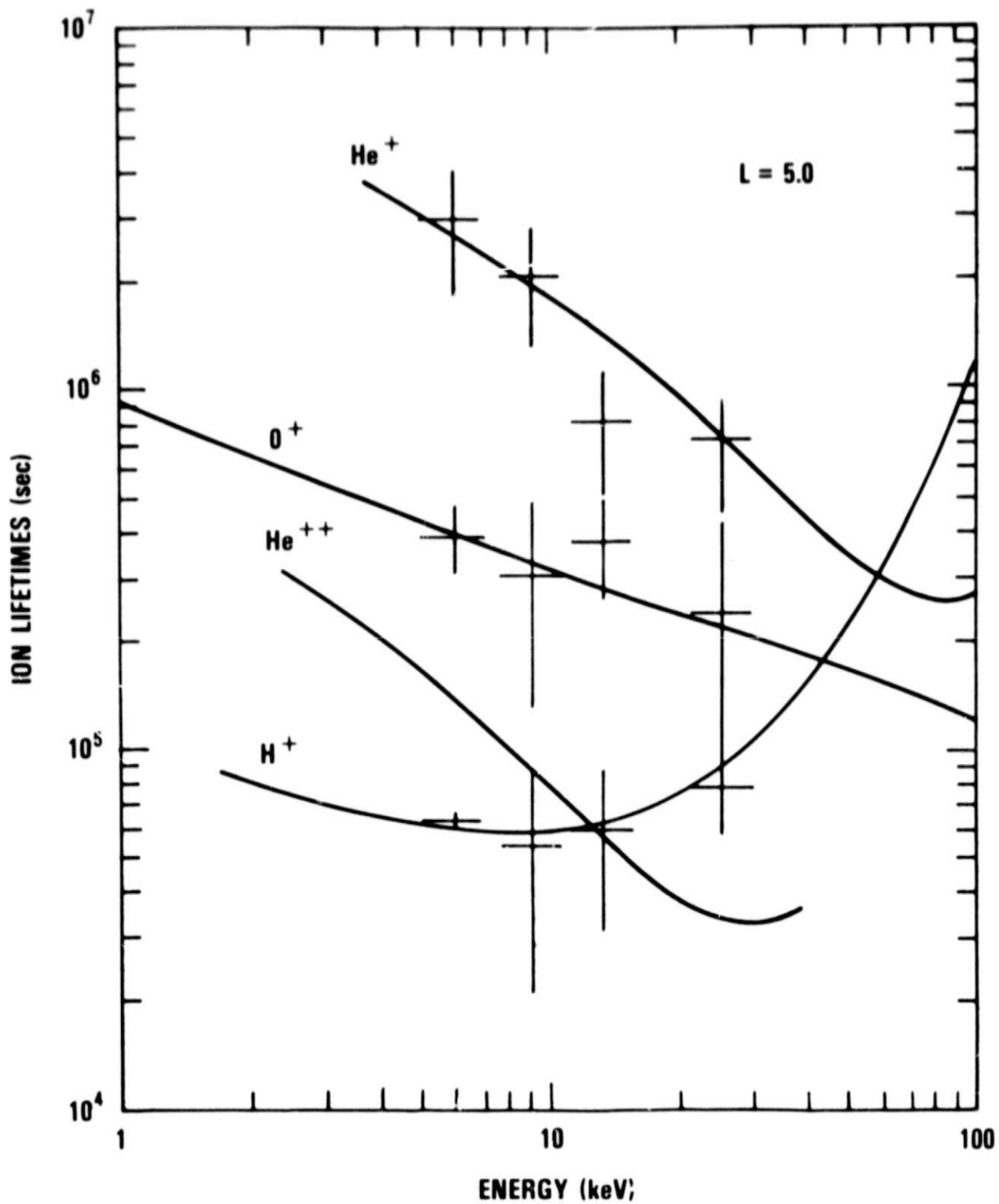


FIGURE 9c